



PERGAMON

International Journal of Solids and Structures 40 (2003) 5175–5185

INTERNATIONAL JOURNAL OF  
**SOLIDS and**  
**STRUCTURES**

[www.elsevier.com/locate/ijsolstr](http://www.elsevier.com/locate/ijsolstr)

## Synchronization of two chaotic oscillators via a negative feedback mechanism

Andrzej Stefański \*, Tomasz Kapitaniak

Division of Dynamics, Technical University of Łódź, Stefanowskiego 1/15, 90-924 Łódź, Poland

Received 10 September 2002; received in revised form 9 January 2003

---

### Abstract

The phenomenon of ideal synchronization of a pair of identical dynamical systems coupled by a one-to-one negative feedback mechanism is described and explained. The theoretical analysis supported by numerical simulations, which is presented in this paper, confirms the properties of chaotic synchronization (in the case of *full coupling*) that have been observed earlier. Additionally, this analysis develops a description of the problem under consideration for *partial coupling* between analyzed dynamical systems. Two classical Lorenz systems and Duffing oscillators coupled by a one-to-one negative feedback mechanism are considered as numerical examples.

© 2003 Elsevier Ltd. All rights reserved.

**Keywords:** Coupled dynamical systems; Chaos synchronization; Lyapunov exponents; Negative feedback coupling

---

### 1. Introduction

The phenomenon of synchronization in dynamical systems has been known for a long time. Recently, the idea of synchronization has been also adopted for chaotic systems. It has been demonstrated that two or more chaotic systems can synchronize by linking them with mutual coupling or with a common signal or signals (Blekhman et al., 1995; Brown et al., 1994; Fujisaka and Yamada, 1983; Kapitaniak, 1994; Pecora and Carroll, 1990, 1991; Pyragas, 1993). In the case of coupled, identical chaotic systems, i.e. the same set of ODEs and values of the system parameters, ideal synchronization can be obtained. The ideal synchronization takes place when all trajectories converge to the same value and remain in step with one another during further evolution (i.e.  $\lim_{t \rightarrow \infty} |x(t) - y(t)| = 0$  for two arbitrarily chosen trajectories  $x(t)$  and  $y(t)$ ). In such a situation, all subsystems of the augmented system evolve on the same manifold on which one of these subsystems evolves (the phase space is reduced to the synchronization manifold). Linking homo-chaotic systems (i.e. systems given by the same set of ODEs but with different values of the system parameters) can lead to practical synchronization (i.e.  $\lim_{t \rightarrow \infty} |x(t) - y(t)| \leq \varepsilon$ , where  $\varepsilon$  is a vector of small parameters) (Kapitaniak et al., 1996; Liu and Rios Leite, 1994). In such linked systems, a significant change

---

\* Corresponding author. Fax: +48-42-6365646.

E-mail address: [steve@ck-sg.p.lodz.pl](mailto:steve@ck-sg.p.lodz.pl) (A. Stefański).

of the chaotic behavior of one or more systems can be also observed. This so-called “controlling chaos by chaos” procedure has some potential importance for mechanical and electrical systems. An attractor of such two systems coupled by a negative feedback mechanism can be even reduced to the fixed point (Fujisaka and Yamada, 1983; Stefański and Kapitaniak, 1996).

This paper concerns the ideal synchronization of two identical dynamical systems coupled by a negative feedback mechanism. When these systems are uncoupled, they work in a chaotic range. This problem has been described earlier by other researchers (Fujisaka and Yamada, 1983) for the case of full symmetrical coupling. In recent authors’ papers, a description of this phenomenon has been developed for the case of non-symmetrical and unidirectional coupling and properties of the ideal synchronization have been applied for the estimation of the largest Lyapunov exponent in non-smooth systems (Stefanśki and Kapitaniak, 2000; Stefanśki, 2000). This method of estimation exploits a property of the linear dependence between the coupling rate and the largest Lyapunov exponent characterizing both identical coupled systems. In this paper, we present a developed analysis of the ideal synchronization process, also for a pair of partially coupled identical oscillators (the definition of *full* and *partial coupling* is to be found in the next section). The theoretical analysis (described in Section 2) is supported by the numerical simulations presented in Section 3. Two classical Lorenz systems and Duffing oscillators coupled by a one-to-one negative feedback mechanism are considered as numerical examples.

## 2. Synchronization via a negative feedback

The dynamical system under consideration is composed of two identical  $n$ -dimensional subsystems coupled by a one-to-one negative feedback mechanism with a pair of coupling coefficients  $d_x$  and  $d_y$ . A scheme of such a system is shown in Fig. 1. The general form of its mathematical description is given by the following first order differential equations:

$$\begin{aligned}\dot{x} &= f(x) + d_x(y - x), \\ \dot{y} &= f(y) + d_y(x - y),\end{aligned}\tag{1}$$

where  $x, y \in \mathbb{R}^n$  ( $n \in \mathbb{N} \geq 3$ ) and  $d_{x,y} = \text{diag}[d_{x,y}; d_{x,y}; \dots; d_{x,y}] \in \mathbb{R}^k \geq 0$ , ( $k = 0, 1, 2, \dots, n$ ) is a diagonal coupling matrix. The natural number  $k$  represents a dimension of the coupling matrix.

Depending on the dimension of the coupling matrix, two forms of coupling can be distinguished, namely:

- (i) *Full coupling*, which is realized by all  $n$ -numbers of first order ODEs describing the connected subsystems. Thus, the dimension of the coupling matrix is equal to the dimension of the phase space of these subsystems ( $k = n$ ).

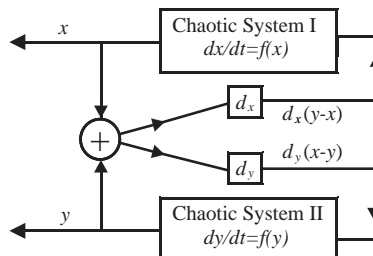


Fig. 1. The scheme of negative feedback coupling mechanism.

(ii) *Partial coupling* where both subsystems are not coupled by all first order ODEs but only by some of them ( $1 \leq k < n$ ).

In the first part of our considerations, let us assume that for  $k = 0$  (lack of coupling) each of the subsystems of the system given by Eq. (1) evolves on the asymptotically stable chaotic attractor  $A$ . In this case the system under consideration (Eq. (1)) is simplified to a pair of separate dynamical systems given by the equations:

$$\begin{aligned}\dot{x} &= f(x), \\ \dot{y} &= f(y).\end{aligned}\tag{2}$$

Since these both systems are identical, it can be assumed that the solutions to both Eq. (2) starting from different initial points of the same basin of attraction, represent two uncorrelated trajectories evolving on the same attractor  $A$  (after a period of the transient motion), so  $x \neq y$ . If initial conditions are the same, the evolution of both the subsystems is identical and we have the ideal synchronization ( $x = y$ ).

Now, we introduce a new variable  $z$  representing the *trajectory separation* between both subsystems during the time evolution. This variable is defined by the expression:

$$z = x - y,\tag{3}$$

where  $z \in \mathbb{R}^n$ . The absolute value of the *trajectory separation*:

$$q = \|\vec{z}\| = |x - y|\tag{4}$$

describes the norm ( $q \in \mathbb{R} \geq 0$ ) of the *trajectory separation* vector:

$$\vec{z} = \vec{x} - \vec{y}.\tag{5}$$

The time variations of the norm of the *trajectory separation* vector are determined by the first time derivative of Eq. (4):

$$\begin{aligned}\dot{q} &= \dot{x} - \dot{y} \quad \text{for } x \geq y, \\ \dot{q} &= \dot{y} - \dot{x} \quad \text{for } x < y,\end{aligned}\tag{6}$$

and, after substituting Eq. (2) into Eq. (6), we obtain:

$$\begin{aligned}\dot{q} &= f(x) - f(y) \quad \text{for } x \geq y, \\ \dot{q} &= f(y) - f(x) \quad \text{for } x < y.\end{aligned}\tag{7}$$

For a small *trajectory separation* vector, that is to say,  $q \ll |A|$ , where  $|A| \in \mathbb{R} \geq 0$  is the attractor's size, i.e. the maximum distance between two points on the attractor in the phase space, we can assume that the distance between trajectories of the subsystems under consideration is given by the linearized equation resulting from the definition of the Lyapunov exponent:

$$q = \delta_0 \exp(\lambda_{\max} t),\tag{8}$$

where  $\lambda_{\max}$  is the largest Lyapunov exponent (positive for the chaotic system),  $\delta_0 \in \mathbb{R} \geq 0$  is an initial (infinitely small) distance between trajectories. The first time derivative of Eq. (8) is given by the relation:

$$\dot{q} = \lambda_{\max} \delta_0 \exp(\lambda_{\max} t).\tag{9}$$

The comparison of Eqs. (7) and (9) yields the equalities:

$$\begin{aligned}x \geq y : f(x) - f(y) &= \lambda_{\max} \delta_0 \exp(\lambda_{\max} t), \\ x < y : f(y) - f(x) &= \lambda_{\max} \delta_0 \exp(\lambda_{\max} t).\end{aligned}\tag{10}$$

Eq. (10) is fulfilled only for a certain time  $\tau \approx (1/\lambda_{\max}) \ln(|A|/\delta_0)$ . After this time, non-linear effects become important.

The next step is an introduction of coupling according to Eq. (1). In the case of *full coupling*, when the equality of dimensions ( $k = n$ ) takes place, we can describe the time evolution of the *trajectory separation* vector norm with the following equations:

$$\begin{aligned} x \geq y : \dot{q} &= f(x) - f(y) - (d_x + d_y)q, \\ x < y : \dot{q} &= f(y) - f(x) - (d_x + d_y)q. \end{aligned} \quad (11)$$

Using Eq. (10) in Eq. (11), we obtain:

$$\frac{dq}{dt} = \lambda_{\max} \delta_0 \exp(\lambda_{\max} t) - (d_x + d_y)q. \quad (12)$$

In order to separate variables, we have to divide Eq. (12) by the expression  $q/dt$  and next use the substitution  $\delta_0 q = \exp(-\lambda_{\max} t)$  arising from Eq. (8). Now, Eq. (12) is given in the form:

$$\frac{dq}{q} = [\lambda_{\max} - (d_x + d_y)]dt, \quad (13)$$

and has the following solution:

$$q = q_0 \exp(\lambda_{\max} t) \exp[(d_x + d_y)t], \quad (14)$$

where  $q_0$  is a norm of the initial *trajectory separation* vector.

From Eq. (14) we see that the *trajectory separation* is the product of two independent factors:

- (i) exponential divergence of nearby trajectories with a rate proportional to the positive Lyapunov exponent, which is given by Eq. (9),
- (ii) exponential convergence due to the introduced negative feedback coupling with a rate proportional to the sum of coupling coefficients. The evolution of the *trajectory separation* associated with this effect can only be described in the form:

$$\frac{dq}{dt} = -(d_x + d_y)q. \quad (15)$$

As results from Eq. (14), the fulfillment of the inequality:

$$d_x + d_y > \lambda_{\max} \quad (16)$$

guarantees the full synchronization because the *trajectory separation* vector decreases to zero.

The first of the above-described phenomena occurs only in the direct neighborhood of the synchronized state where linear effects are dominant. The second one acts in the entire phase space. For that reason, the product of both exponential effects (Eq. (14)) takes place only nearby the synchronization manifold.

In further analysis, to simplify the visualization, we took  $n = 3$  and assumed that the evolution on the attractor  $A$  was characterized by one positive Lyapunov exponent.

The two-dimensional visualization of the first of the above-mentioned exponential effects is shown in Fig. 2(a). The Lyapunov exponents are related to the expanding or contracting nature of different directions in the phase space and the number of them is equal to the phase space dimension. In the example shown in Fig. 2(a), we have assumed that the perpendicular axes of  $z$ -directions (*trajectory separation* vector) are covered with the principal axes associated with a given Lyapunov exponent. Thus, the axis  $z_1$  represents the expanding direction of the phase space connected with the positive Lyapunov exponent ( $\lambda_{\max} > 0$ ) and the axis  $z_2$  is associated with the contracting direction ( $\lambda_{\min} < 0$ ). The direction corresponding to the exponent  $\lambda = 0$  is always tangential to the phase trajectory. Such expanding and contracting effects cause that during

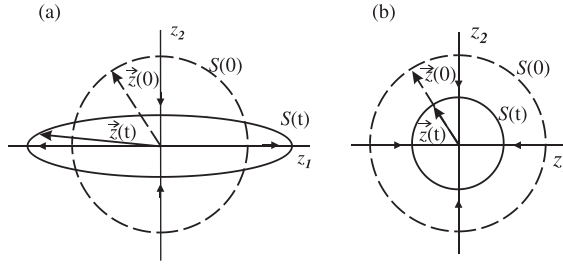


Fig. 2. Two-dimensional images of positive Lyapunov exponent effect (a) and negative feedback coupling effect (b).

the time evolution the infinitesimal sphere of initial conditions  $S(0)$  (interrupted line) is deformed into the ellipsoid  $S(t)$  (solid line). Also the initial *trajectory separation* vector  $\vec{z}(0)$  increases at a rate proportional to the largest Lyapunov exponent.

In Fig. 2(b) the visualization of the influence of a negative feedback on the evolution of the *trajectory separation* vector and the sphere of initial conditions  $S(0)$  in the phase space of the system represented by Eq. (15) is shown. This figure shows that *full coupling* has a convergent nature and causes a permanent decrease of the *trajectory separation* vector at a rate proportional to the sum of coupling coefficients. For the same reason, the volume of the sphere  $S(t)$  diminishes during the time evolution but this sphere is not deformed because the process described by Eq. (15) has a linear character.

The assumed covering of the  $z$ -direction and principal  $\lambda$ -direction axes does not take place in reality. The spatial orientation of the system of coordinates associated with a given Lyapunov exponent varies in a complex way during the evolution on the attractor. But in Fig. 2(a) it is shown that the negative feedback acts in all directions of the phase space with the same rate. Therefore, in the case of *full coupling*, inequality (16) is always fulfilled in spite of the disagreement of the principal directions of both the exponential effects. Thus, inequality (16) is the condition of the full synchronization of the two fully coupled identical dynamical systems given by Eq. (1).

However, the condition of synchronization given by inequality (16) does not ensure the full synchronization in a situation when only *partial coupling* is applied. In such a case, coupling is not realized by one or more first order ODEs describing the connected systems ( $k < n$ ). This fact causes that the effect of a negative feedback may not have such a regular nature as it is shown in Fig. 2(b) and the dependence between the sum of coupling coefficients and the largest Lyapunov exponent (inequality (16)) may not be fulfilled. In order to estimate the effectiveness of *partial coupling*, we have introduced the coefficient of coupling effectiveness  $\kappa$ . The idea of this coefficient is illustrated by the following inequality:

$$d_x + d_y > \kappa \lambda_{\max}, \quad (17)$$

which is the condition of synchronization for partially coupled chaotic oscillators ( $\kappa \in \mathbb{R} > 0$ ).

The above-presented mathematical analysis concerns the chaotic synchronization by *full coupling*, for which the value of the coefficient  $\kappa$  amounts to 1 and it is defined only for the largest positive Lyapunov exponents ( $\lambda_{\max} > 0$ ). The analytical determination of this coefficient for *partial coupling* is very difficult or even impossible. However, it can be estimated in a way of numerical investigations of the full synchronization process, according to the relation:

$$\kappa = \frac{D_s}{\lambda_{\max}}, \quad (18)$$

where  $D_s$  is the smallest value of the sum of coupling coefficients ( $d_x + d_y$ ) for which stable synchronized motion appears.

### 3. Numerical simulations

In this section we present the examples of numerical analysis of double chaotic oscillators given by Eq. (1). All numerical simulations have been carried out with the DYNAMICS (Nusse and Yorke, 1997) and INSITE (Parker and Chua, 1989) software. As the examples of chaotic systems, two classical non-linear oscillators have been applied, namely:

- (i) Duffing oscillator,
- (ii) Lorenz system.

#### 3.1. Coupled Duffing oscillators

In the first part of this section, we present numerically simulated synchronization of two coupled, identical Duffing oscillators working in chaotic regime. A single Duffing system is described by the well-known equation of motion:

$$m\ddot{x} - kx(1 - x^2) + c\dot{x} = F \cos(\omega t), \quad (19)$$

where  $m$  is the mass of the oscillator,  $k(1 - x^2)$  the non-linear stiffness of the spring,  $c$  the coefficient of viscous damping,  $F$  the amplitude of the harmonic exciting force,  $\omega$  the frequency of forcing. In the numerical analysis, the same values of system parameters were assumed for all the cases considered.

In the first case under consideration, two oscillators (Eq. (19)) are coupled together according to Eq. (1) by a *full coupling* mechanism. Dividing Eq. (19) by the mass  $m$  and introducing the substitutions:  $x = x_1$ ,  $\dot{x} = x_2$ ,  $a = k/m$ ,  $h = c/m$ ,  $p = F/m$  and putting in Eq. (1), we obtain the augmented system in the following form:

$$\begin{aligned} \dot{x}_1 &= x_2 + d_x(y_1 - x_1), \\ \dot{x}_2 &= p \cos(\omega t) + ax_1(1 - x_1^2) - hx_2 + d_x(y_2 - x_2), \\ \dot{y}_1 &= y_2 + d_y(x_1 - y_1), \\ \dot{y}_2 &= p \cos(\omega t) + ay_1(1 - y_1^2) - hy_2 + d_y(x_2 - y_2). \end{aligned} \quad (20)$$

Two forms of *full coupling* have been considered during the numerical analysis: symmetrical coupling ( $d_x = d_y = d$ ) and unidirectional coupling ( $d_x = d$ ,  $d_y = 0$ ). According to the condition of synchronization (inequality (16)), this phenomenon should take place when the sum of coupling parameters exceeds the largest Lyapunov exponent which is characteristic of the systems coupled in Eq. (20). It is confirmed by the bifurcation diagrams shown in Fig. 3(a) and (b), where we can see that synchronization appears (*trajectory separation*  $z_1 = x_1 - y_1$  tends to zero) for the smallest value of parameter  $d$  (synchronization value  $d_s$  in further considerations) predicted by inequality (16), i.e. it is approximated by the largest Lyapunov exponent (given on the top of the figures) for unidirectional coupling ( $\lambda_{\max} \approx D_s = d_s$ , see Fig. 3(b)) or half of this value for symmetrical coupling ( $\lambda_{\max} \approx D_s = 2d_s$ , see Fig. 3(a)). However, *full coupling* has no real equivalent because it is impossible to execute such kind of coupling (given by Eq. (20)) in a real mechanical system. It can be done with numerical simulations only.

However, an equivalent in reality has *partial coupling* in the form described by the following equations:

$$\begin{aligned} \dot{x}_1 &= x_2, \\ \dot{x}_2 &= p \cos(\omega t) + ax_1(1 - x_1^2) - hx_2 + d_x(y_2 - x_2), \\ \dot{y}_1 &= y_2, \\ \dot{y}_2 &= p \cos(\omega t) + ay_1(1 - y_1^2) - hy_2 + d_y(x_2 - y_2). \end{aligned} \quad (21)$$

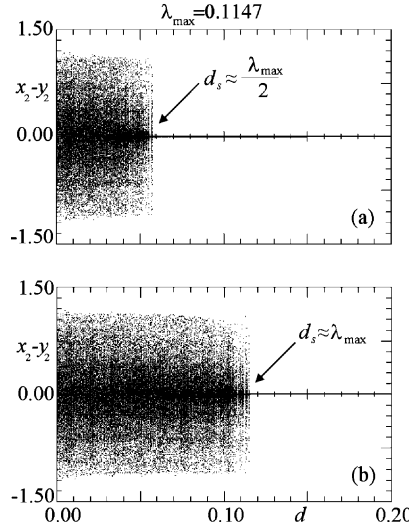


Fig. 3. The bifurcation diagrams of *trajectory separation* versus coupling coefficient  $d$  for *full coupling* (Eq. (20)) of two chaotic Duffing oscillators: (a) symmetrically coupled ( $d_x = d_y = d$ ), (b) unidirectionally coupled ( $d_x = d$ ,  $d_y = 0$ );  $a = 1.00$ ,  $h = 0.25$ ,  $p = 0.30$ ,  $\omega = 1.00$ . The corresponding value of the largest Lyapunov exponent—on the top.

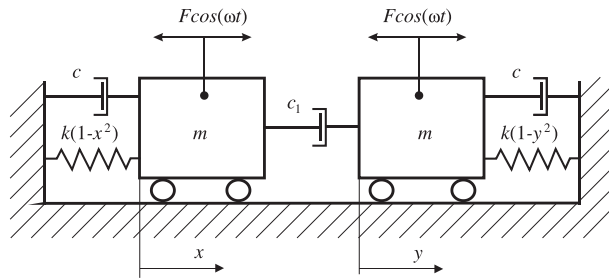


Fig. 4. Coupled Duffing oscillators.

The physical model of the system given by Eq. (21) is shown in Fig. 4. The coupling between vibrating masses is symmetrical ( $d_x = d_y = d$ ) and it is realized by a viscous damper with the damping coefficient  $c_1$ . The coupling parameter represents the damping rate between both masses ( $d = c_1/m$ ). The results of the numerical modelling of *partial coupling* according to Eq. (21) are presented in Fig. 5(a) and (b). These figures illustrate the bifurcation diagrams of the *trajectory separation* versus the coupling coefficient of two identical numerical models of the analysed system, starting from different initial conditions. It is clearly visible that in both examples, synchronization appears for approximately the same value of the coupling parameter, thus synchronization by *partial coupling* is not an accidental process. Dividing the double synchronization value  $d_s$  by the largest Lyapunov exponent, we can estimate the value of coupling effectiveness according to Eq. (18) ( $\kappa \approx 2.30$ ). The effectiveness of both the coupling forms is also exemplified by a comparison of Fig. 5(a) and (b) with the analogous one shown in Fig. 3(a).

### 3.2. Coupled Lorenz systems

The second numerical example has been carried out on the basis of coupled chaotic Lorenz oscillators. Substituting the Lorenz system in Eq. (1), the augmented system is given in the form:

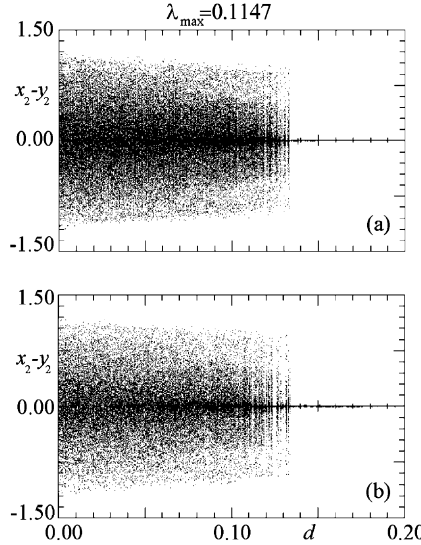


Fig. 5. The bifurcation diagrams of *trajectory separation* versus coupling coefficient  $d$  for *partial coupling* (Eq. (21)) of two chaotic Duffing oscillators (analogous to these shown in Fig. 3(a) and (b)) starting from different initial conditions in each step of bifurcation parameter: (a)  $x_1(0) = 1.00$ ,  $x_2(0) = 0.00$ ,  $y_1(0) = 0.00$ ,  $y_2(0) = 1.00$ , (b)  $x_1(0) = -1.00$ ,  $x_2(0) = 1.00$ ,  $y_1(0) = 3.00$ ,  $y_2(0) = 2.00$ .

$$\begin{aligned}
 \dot{x}_1 &= -\delta(x_1 - x_2) + d_{x1}(y_1 - x_1), \\
 \dot{x}_2 &= -x_1x_3 + rx_1 - x_2 + d_{x2}(y_2 - x_2), \\
 \dot{x}_3 &= x_1x_2 - bx_3 + d_{x3}(y_3 - x_3), \\
 \dot{y}_1 &= -\delta(y_1 - y_2) + d_{y1}(x_1 - y_1), \\
 \dot{y}_2 &= -y_1y_3 + ry_1 - y_2 + d_{y2}(x_2 - y_2), \\
 \dot{y}_3 &= y_1y_2 - by_3 + d_{y3}(x_3 - y_3),
 \end{aligned} \tag{22}$$

where  $\delta$ ,  $b$  and  $r$  are the system parameters and  $\text{diag}[d_{x,y1}, d_{x,y2}, d_{x,y3}]$  is the coupling matrix.

During the numerical simulations, three forms of symmetrical coupling were considered:

- (i) *full coupling* ( $d_{x,y1} = d_{x,y2} = d_{x,y3} = d$ ),
- (ii) *partial coupling I* ( $d_{x,y1} = 0$ ,  $d_{x,y2} = d_{x,y3} = d$ ),
- (iii) *partial coupling II* ( $d_{x,y1} = d_{x,y2} = 0$ ,  $d_{x,y3} = d$ ).

The numerically generated synchronization values  $d_s$  for all the above-mentioned cases of coupling are presented on the bifurcation diagrams shown in Fig. 6(a)–(c). Fig. 6(a) shows that, like in the previous example, the effectiveness of *full coupling* is about 1 ( $\lambda_{\max} \approx D_s = 2d_s$ ). However, as we can see in Fig. 6(b) and (c), *partial coupling* can be less ( $\kappa \approx 1.25$ , see Fig. 6(c)) as well as even more effective ( $\kappa \approx 0.93$ , see Fig. 6(b)) than its full version.

#### 4. Discussion and conclusions

The theoretical analysis presented in this paper demonstrates an existence of the close dependance between synchronization of identical chaotic systems and the largest Lyapunov exponent if *full coupling* is

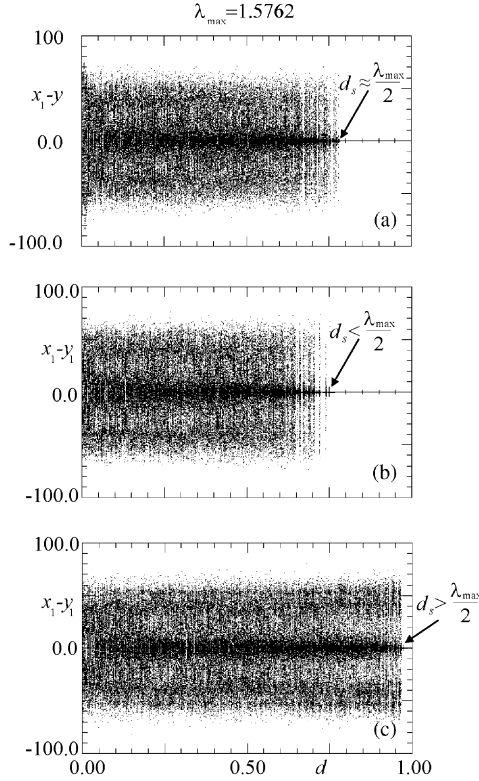


Fig. 6. The bifurcation diagrams of *trajectory separation* versus coupling coefficient  $d$  for coupled chaotic Lorenz systems (Eq. (22)): (a) *full coupling* ( $d_{x,y1} = d_{x,y2} = d_{x,y3} = d$ ), (b) *partial coupling I* ( $d_{x,y1} = 0, d_{x,y2} = d_{x,y3} = d$ ), (c) *partial coupling II* ( $d_{x,y1} = d_{x,y2} = 0, d_{x,y3} = d$ );  $\delta = 10.0, b = 8/3, r = 120.0$ . The corresponding value of the largest Lyapunov exponent—on the top.

applied to them. Such dependance can be used in practice. Namely, the above-mentioned properties of chaos synchronization via *full coupling* allow us to estimate the largest Lyapunov exponent of an arbitrary system (Stefaniński and Kapitaniak, 2000; Stefaniński, 2000). The method based on these properties can be very useful for non-smooth systems, where the estimation of Lyapunov exponents is not straightforward. For smooth systems, it can be the way to verify the results obtained by means of the classical algorithm.

However, in the case of *partial coupling* of two mechanical systems, the linear dependance between the synchronization rate of coupling and the largest Lyapunov exponent is not fulfilled in most cases ( $\kappa \neq 1$ ). Such coupling is not executed by all first order ODEs describing coupled systems. For that reason, the real effect of negative feedback does not have such a regular influence on synchronization as the effect of *full coupling*. The real condition of synchronization is more complicated. Therefore, we have introduced the coefficient  $\kappa$  in order to describe the effectiveness of *partial coupling*. In all the cases considered in this paper, the value of the coefficient  $\kappa$  is independent of initial conditions (see the examples shown in Fig. 5(a) and (b)). Possible influence of initial conditions on the effectiveness of *partial coupling* has not been found in the systems under analysis.

The additional visualization of both forms of coupling is given by the comparison of the Lyapunov exponents for *full* and *partial coupling*, which is presented in Fig. 7(a) and (b). These figures illustrate the bifurcation diagrams of the four largest Lyapunov exponents corresponding to Fig. 6(a) (*full coupling* Fig. 7(a)) and Fig. 6(b) (*partial coupling I*, Fig. 7(b)), respectively. Comparing Fig. 6(a) and (b) with Fig. 7(a) and (b), we can observe that synchronization occurs when the exponent  $\lambda_2$  becomes negative. This fact

shows an another aspect of chaotic synchronization. Namely, this phenomenon can be considered (in the cases presented) as a process of the transition from hyperchaotic motion in the  $2n$ -dimensional phase space (with two positive Lyapunov exponents) to chaotic motion (with one positive Lyapunov exponent) on the  $n$ -dimensional synchronization manifold  $x = y$ . Obviously, such process does not always lead to synchronization because it is also possible that after the transition from hyperchaos, the chaotic attractor is not locked on the synchronization subspace.

It is clearly visible in Fig. 7(a), as well as in Figs. 3(a) and (b) and 6(a), that the regular nature of *full coupling* shown in Fig. 2(a) always forces the transition to synchronization, according to the condition given by inequality (16) ( $d_s \approx \lambda_{\max}/2$ , so  $\kappa \approx 1$ ) and makes the anticipation of the synchronization process (if the largest Lyapunov exponent is known) possible. In the case of *partial coupling*, the convergence is irregular because such coupling does not act in all directions of the phase space with the same rate, hence it does not ensure satisfying inequality (16). The connection of such a form of convergence with the effect of non-linearity in the hyperchaotic regime makes it impossible to predict the level of coupling effectiveness  $\kappa$ . From the viewpoint of the analysis presented in Section 2, *full coupling* seems to be the most effective ( $\kappa = 1$ ). Thus, *partial coupling* should not lead to full synchronization for the value of the parameter  $\kappa$  smaller than 1. However, this conjecture is not always valid in practice (what is clearly demonstrated in Figs. 7(b) and 6(b) where  $d_s < \lambda_{\max}/2$ ), due to the above-mentioned unpredictable behavior of partially coupled systems in the desynchronized state on the hyperchaotic attractor.

This short discussion touches on the problem under consideration only in general. Especially, the phenomenon of high effectiveness of *partial coupling* (in the cases when  $\kappa < 1$ ) requires more detailed explanation, which is our task for the future and will be reported later.

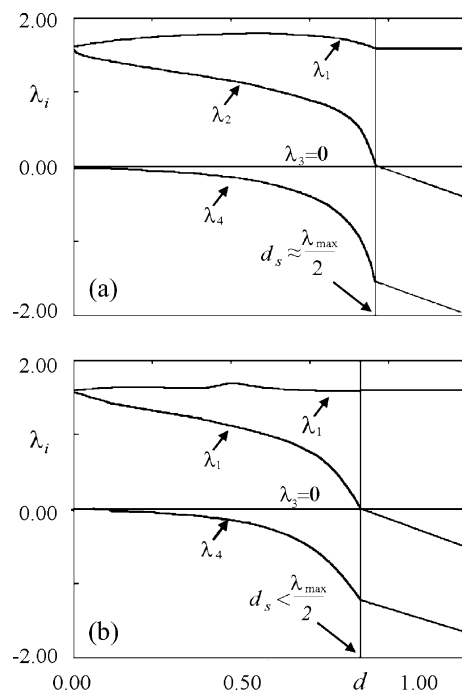


Fig. 7. Variation of the largest Lyapunov exponents versus coupling coefficient  $d$  for coupled Lorenz systems (Eq. (22)) corresponding to: (a) *full coupling* (Fig. 6(a)); (b) *partial coupling* (Fig. 6(b)).

## Acknowledgement

This study has been supported by the Polish Committee for Scientific Research (KBN) under project no. 5 T07A 014 23.

## References

Blekhan, I., Landa, P.S., Rosenblum, M.G., 1995. Synchronization and chaotization in interacting dynamical systems. *Appl. Mech. Rev.* 48, 733–752.

Brown, R., Rulkov, H.F., Tufillaro, N.B., 1994. The effects of additive noise and drift in the dynamics of the driving on chaotic synchronization. *Physics Letters A* 196, 201–205.

Fujisaka, H., Yamada, T., 1983. Stability theory of synchronized motion in coupled oscillator systems. *Progress of Theoretical Physics* 69, 32–47.

Kapitaniak, T., 1994. Synchronization of chaos using continuous control. *Physical Review E* 50, 1642–1644.

Kapitaniak, T., Sekieta, M., Ogorzałek, M., 1996. Monotone synchronization of chaos. *Int. J. Bifurcation and Chaos* 6, 211–217.

Liu, Y., Rios Leite, J.R., 1994. Coupling of two chaotic lasers. *Physics Letters A* 191, 134–138.

Nusse, H.E., Yorke, J.A., 1997. *Dynamics: Numerical Explorations*. Springer-Verlag, New York.

Parker, T.S., Chua, L.O., 1989. *Practical numerical algorithms for chaotic systems*. Springer-Verlag, Berlin.

Pecora, L.M., Carroll, T.L., 1990. Synchronization in chaotic systems. *Physical Review Letters* 64, 821–824.

Pecora, L.M., Carroll, T.L., 1991. Driving systems with chaotic signals. *Physical Review A* 44, 2374–2383.

Pyragas, K., 1993. Predictable chaos in slightly perturbed unpredictable chaotic systems. *Physics Letters A* 181, 203–208.

Stefański, A., 2000. Estimation of the largest Lyapunov exponent in systems with impacts. *Chaos Solitons and Fractals* 11, 2443–2451.

Stefański, A., Kapitaniak, T., 1996. Steady state locking in coupled chaotic systems. *Physics Letters A* 210, 279–282.

Stefański, A., Kapitaniak, T., 2000. Using chaos synchronization to estimate the largest Lyapunov exponent of non-smooth systems. *Discrete Dynamics in Nature and Society* 4, 207–215.